Contents lists available at ScienceDirect

Photonics and Nanostructures - Fundamentals and

journal homepage: http://ees.elsevier.com

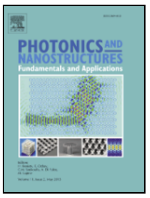

A simple analytic approach to the problem of excitation of surface plasmon polaritons with a dipole nanoantenna

Anton V. Dyshlyuk [a,*], Andrey A. Bogdanov [b], Oleg B. Vitrik [c]

[a] Institute of Automation and Control Processes (IACP) FEB RAS, Far Eastern Federal University (FEFU) and Vladivostok State University of Economics and Service (VSUES), Vladivostok, Russia
[b] ITMO University, Saint Petersburg, Russia
[c] Institute of Automation and Control Processes (IACP) FEB RAS, Far Eastern Federal University (FEFU), Russia

ARTICLE INFO

Keywords
SPP
Surface plasmon polaritons
Nanoantenna
SPP excitation

ABSTRACT

Surface plasmon polaritons can be efficiently excited using attenuated total internal reflection techniques or with diffraction gratings. An alternative way actively studied in recent years is the use of nanoantennas. Here, we show that the amplitude of surface plasmon polariton excited by a nanoantenna can be found analytically using a well-known method for calculation of guided-mode amplitudes in the presence of current sources, which is widely used in the waveguide theory. The calculations are carried out for the simplest 2D case of an infinitely long cylindrical rod of a small radius illuminated by a plane wave and placed in the vicinity of metal substrate parallel to its interface. The validity of the analytical solution is confirmed by the results of numerical simulations.

1. Introduction

Surface plasmon polaritons (SPPs) are surface electromagnetic waves arising from the coupling of photons with electron plasma oscillations at the interface between a dielectric and a metal or highly doped semiconductor. They were first observed experimentally by R. Wood in 1901 [1] as anomalies in the reflectance spectra of metal gratings. The correct interpretation of the anomalies as the excitation of surface waves was given by U. Fano in 1941 [2]. However, he didn't gain deeper insight into the nature of these waves. More detailed analysis in terms of surface plasma oscillations was introduced by R. Ritchie in [3].

The electromagnetic field of SPP decays exponentially away from the interface and becomes extremely localized at the resonant frequency. This makes the use of SPP a very promising strategy towards miniaturization of optical integrated circuits. In particular, plasmonic waveguides are capable of squeezing light at telecommunication frequencies down to the nanoscale [4,5]. Plasmonic waveguides are used, for example, for subwavelength imaging [6] and in commercially available quantum cascade lasers [7,8]. Tight spatial localization of light in plasmonic structures is accompanied by a giant amplification of the incident field, which opens up exciting opportunities for biosensing [9–11], nonlinear optics [12–14], Raman spectroscopy [15,16], and enhancement of light-mater interaction [17,18]. Plasmon excitations are well-studied in both extended and localized structures. To learn more about SPPs we refer the reader to the following monographs and reviews: [19–24].

Being a surface wave, SPP cannot be excited from free space by a plane wave because of the in-plane momentum mismatch. Usually, to provide matching between in-plane momenta of SPP and incident light, grating couplers [25], high-refractive-index prisms (Otto or Kretschmann configurations) [26,27] or other defects (grooves, holes, notches, etc) breaking the in-plane translation symmetry are used [28–30]. An alternative method to excite SPPs is to use dielectric or plasmonic nanoantennas [31–34]. Due to their resonant properties, the excitation of SPPs can be very efficient [35–37]. Moreover, the interference between different multipole moments of the nanoantenna provides efficient dynamical control over the directivity of SPP [38] so that it can be used for SPP demultiplexing on a chip [39].

The scattering problem of a small nanoparticle on a metal substrate illuminated by a plane wave can be solved analytically in a dipole approximation using the dyadic Green's function formalism [40,41]. The amplitude of the SPP wave can be extracted by calculating the residue at the pole of the Fresnel reflection coefficient. This method gives a good agreement with the full-wave numerical simulations but it is rather cumbersome and requires the evaluation of the Sommerfeld integrals.

In this work, we present a simple alternative way to calculate the contribution of SPPs to the total field scattered by a plasmonic nanoantenna on a metal substrate. Our method uses the reciprocity theorem and mode orthogonality and is similar to that used in the waveguide

* Corresponding author.
E-mail addresses: anton_dys@iacp.dvo.ru (A.V. Dyshlyuk); bogdan.taurus@gmail.com (A.A. Bogdanov); oleg_vitrik@mail.ru (O.B. Vitrik)

https://doi.org/10.1016/j.photonics.2021.100895
Received 21 June 2020; Received in revised form 24 November 2020; Accepted 7 January 2021
Available online xxx
1569-4410/

theory for calculating the amplitude of the modes excited by a current distribution. To demonstrate the efficiency of the proposed method most clearly we consider a two-dimensional problem, where the SPP mode is excited by an infinitely long cylindrical antenna with a small radius. Firstly, we shall obtain the solution for the case when the antenna has an explicitly defined transverse harmonically oscillating dipole moment. As a second step, we consider the case of illuminating the antenna by a normally incident plane wave polarized perpendicular to its axis. We then validate our analytical approach by numerical simulations in COMSOL Multiphysics software.

2. SPP excitation by a dipole source with an explicitly defined dipole moment

Let us put a source of radiation in the form of a very thin rod at height x_0 above the surface of the metal film with $\varepsilon = \varepsilon_{Me}$ (Fig. 1). The medium above the film is assumed to be a dielectric with $\varepsilon = \varepsilon_D$. We consider the film to be sufficiently thick (much thicker than the skin depth, which is about 15 nm for the noble metals in the visible and near-infrared regions) so that the surface plasmon polaritons are excited only at the upper surface of the film. The rod is assumed to be infinitely long in the y-axis direction (i.e. perpendicularly to the plane of the figure), and its dipole moment per unit length is defined explicitly as $\boldsymbol{p_0}/l$, where the dipole moment vector $\boldsymbol{p_0}$ is parallel to the z-axis and implicitly includes a time dependence of the form $e^{-i\omega t}$. If the diameter of the rod is assumed to be infinitesimal, the current density in the rod can be written as $\boldsymbol{J} = i\omega \boldsymbol{p}_0 l^{-1}\delta(x - x_0)\delta(z)$. To calculate the amplitude of the SPP mode excited by such a source at the surface of the film we use the following expression derived from the unconjugated reciprocity theorem [42]:

$$a = -\frac{1}{4N_C}\int_{(V)} \boldsymbol{e}\cdot\boldsymbol{J}e^{-i\beta z}dV \tag{1}$$

In this expression β and $N_C = \frac{1}{2}\left|\int_S \boldsymbol{e}\times\boldsymbol{h}\cdot\boldsymbol{n}_z dS\right|$ are the propagation constant and mode normalization, respectively; $\boldsymbol{n_z}$ is the unit vector in the direction of the z-axis; $\boldsymbol{e}$, $\boldsymbol{h}$ are the vector electric and magnetic field distributions of a mode in the cross section (S) of the waveguide; V is the volume occupied by the current source. Generally speaking, expression (1) links amplitude a of a dielectric waveguide mode with excitation current density $\boldsymbol{J}$. But in its derivation no restrictions are imposed on the conductivity of the waveguide medium [42], which makes it possible to generalize it to the case of plasmonic waveguides.

The components of the $\boldsymbol{e}$ and $\boldsymbol{h}$ vectors and other parameters of the SPP mode required for the calculation of its amplitude are given as follows [43]:

$$e_z = iA\gamma_{Vac}\cdot X_0(x)(\omega\varepsilon_0\varepsilon_D)^{-1},\quad e_x = -A\beta\cdot X_0(x)\eta_\varepsilon(x)(\omega\varepsilon_0)^{-1},\quad h_y = ,$$

$$X_0(x) = \begin{cases} exp(-\gamma_{Vac}x), & x \geq 0 \\ exp(\gamma_{Me}x), & x < 0 \end{cases},\quad \eta_\varepsilon(x) = \begin{cases} 1/\varepsilon_D, & x \geq 0 \\ 1/\varepsilon_{Me}, & x < 0 \end{cases},\quad \gamma_{Vac} =$$

$$\gamma_{Vac} = ik\varepsilon_D(\varepsilon_{Me}+\varepsilon_D)^{-1/2},\quad \gamma_{Me} = ik\varepsilon_{Me}(\varepsilon_{Me}+\varepsilon_D)^{-1/2},\quad \beta = k(\varepsilon_{Me}\varepsilon_D/$$

where A is an arbitrary constant with the dimensions of A/m. In our case, with the "point" current oscillating in the z direction, the integration of expression (1) yields: $-\frac{\omega p_0}{Al}\gamma_{Vac}\left|\frac{\varepsilon_{Me}^{3/2}\varepsilon_D^{3/2}}{\varepsilon_{Me}^2+\varepsilon_D^2}\right|e^{-\gamma_{Vac}x_0}$.

It is convenient to recast the electric ($\boldsymbol{E^{SPP}} = a\cdot\boldsymbol{e}$) and magnetic ($\boldsymbol{H^{SPP}} = a\cdot\boldsymbol{h}$) fields the excited SPP mode in the form $E_i^{SPP} = E_{0i}^{SPP}X_0(x)e^{-i\beta z}$ and $H_i^{SPP} = H_{0i}^{SPP}X_0(x)e^{-i\beta z}$, where subscript i takes on values x, y, z and coefficients E_{0i}^{SPP} and H_{0i}^{SPP} represent the amplitudes of the electric and magnetic fields of the SPP wave.

For example, the non-zero z- and x-components the electric field amplitude can be written, using the above expression for parameter a, as

$$E_{0z}^{SPP} = -p_0 l^{-1}\frac{\gamma_{Vac}^2}{\varepsilon_0\varepsilon_D}\left|\frac{\varepsilon_{Me}^{3/2}\varepsilon_D^{3/2}}{\varepsilon_{Me}^2+\varepsilon_D^2}\right|e^{-\gamma_{Vac}x_0} \tag{2}$$

$$E_{0x}^{SPP}\Big|_{x=\pm 0} = -\sqrt{\varepsilon_{Me}/\varepsilon_D}\,\eta_\varepsilon(\pm 0)p_0 l^{-1}\frac{\gamma_{Vac}^2}{\varepsilon_0}\left|\frac{\varepsilon_{Me}^{3/2}\varepsilon_D^{3/2}}{\varepsilon_{Me}^2+\varepsilon_D^2}\right|e^{-\gamma_{Vac}x_0}$$

Throughout subsequent calculations we will assume for simplicity that the medium above the metal film is vacuum i.e. $\varepsilon_D = 1$. We plot as solid curves in Fig. 2 the dependences of the E_{0z}^{SPP} component on the excitation wavelength for the case of gold film, $p_0 l^{-1} = 10^{-24}$ C and different values of x_0.

The numerical study of SPP excitation by the source under consideration was carried out with the Finite Element in Frequency Domain

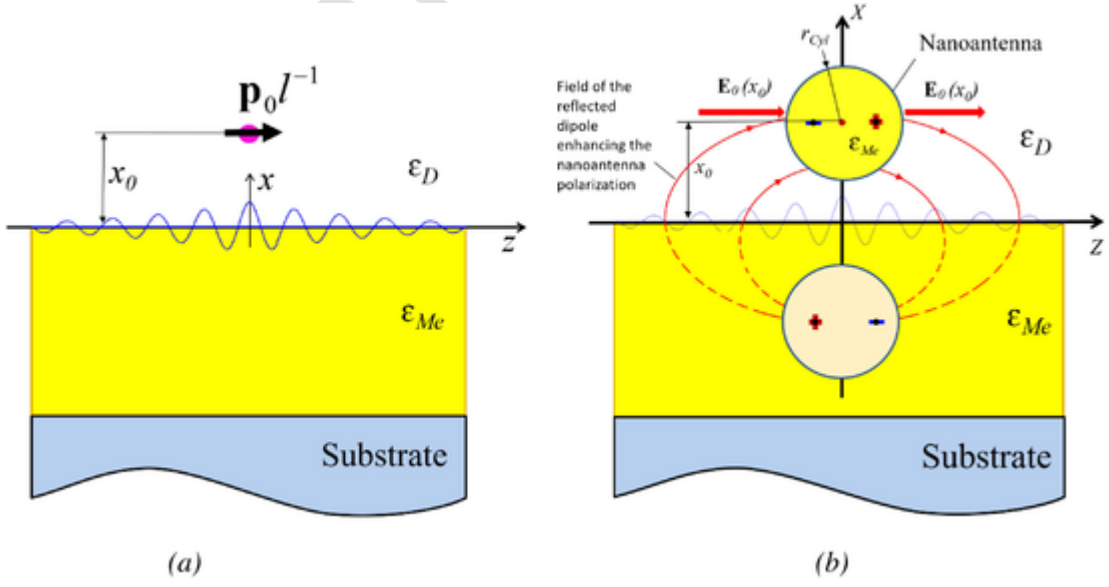

Fig. 1. Excitation of SPP on a metal film: (a) By a "point-like" 2D dipole. The magnitude of the dipole moment per unit length is explicitly defined and is independent of external factors. (b) By a cylindrical nanoantenna. The cylindrical rod is affected by the total field of the incident and reflected waves as well as the field due to the image charges in the substrate, which give rise to the surface dressing effect.

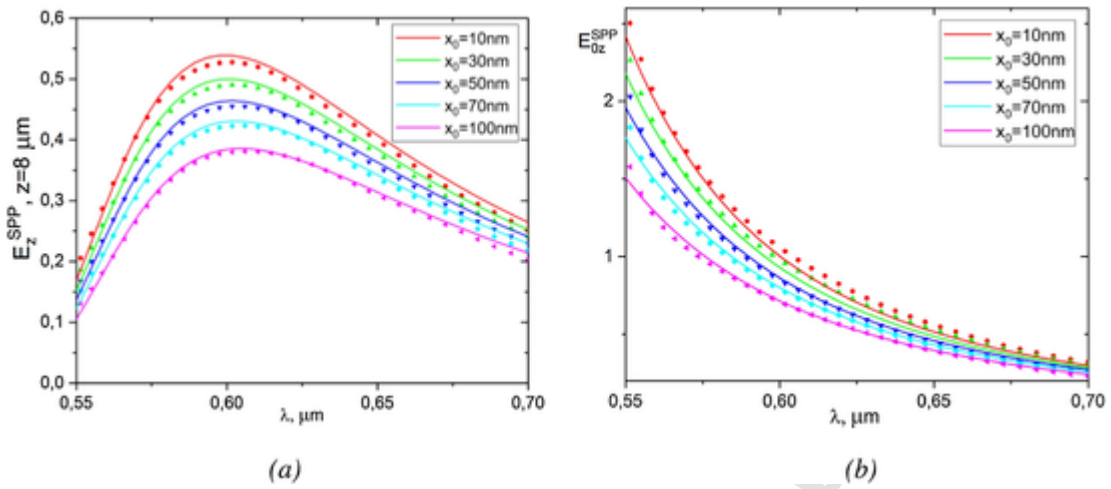

Fig. 2. Comparison of numerically (points) and analytically (solid curves) calculated amplitudes of the longitudinal component of the SPP field at z = 8 μm (a) and z = 0 μm (b) for various heights (x_0) of the source and $\varepsilon_D = 1$.

(FEFD) method using COMSOL Multiphysics software. We applied the "perfectly matched layer" (PML) condition to the exterior boundary of the computational domain, and used mesh refinement in the region between the source and surface of the film, as well as large enough computational domain to ensure convergence of the numerical solution. The complex permittivity data for gold were taken from the CRC handbook [45]. The wavelength range for the simulation was chosen in the visible and near infrared regions from 400 to 700 nm.

The numerically obtained distribution of the electromagnetic field is a superposition of the near field of the dipole source, its radiation field, and the excited SPP mode. It is reasonable to assume that in the chosen spectral range the contributions of the first two components will fall off quickly with distance from the source. At the same time, in the long-wavelength part of the spectrum where the SPP mode has a relatively low attenuation coefficient [43], it can be expected to retain a sizable amplitude even at a considerable distance from the source. Indeed, the numerical results show that a complex dependence of the amplitude of the total electric field on the z-coordinate (at $x = 0$) acquires a purely exponential character for $z > 8$ um and $\lambda > 550$ nm with the attenuation rate given by the imaginary part of the SPP propagation constant calculated analytically in accordance with [43]. This proves that under the above conditions, the SPP mode dominates in the total field on the metal film surface, which makes it possible to estimate its initial amplitude by extrapolation to the point with coordinates $z = 0$, $x = 0$ using the known exponential law of SPP propagation [43].

The numerically calculated spectral dependences of the amplitude of the z-component of SPP electric field for various values of x_0 are shown with points in Fig. 2. The results in Fig. 2(a) correspond to the SPP amplitude at a point with coordinates $z = 8$ μm, $x = 0$, while those in Fig. 2(b) are for the extrapolated initial SPP amplitude at $z = 0$, $x = 0$. As seen from the figures, both directly obtained numerical results and those extrapolated to the origin are in good agreement with the analytical results. This confirms the validity of our analytical approach to the calculation of the SPP mode amplitude.

3. SPP excitation by a 2D cylindrical nanoantenna

Let us now consider the case of SPP excitation by a cylindrical nanoantenna in the form of a thin and very long metal rod of circular cross-section ($r_{Cyl} \ll \lambda$, $l_{Cyl} \gg \lambda$, where r_{Cyl} and l_{Cyl} are the radius and length of the rod, respectively, and λ is the wavelength of illumination) placed at height x_0 above the surface of the film of the same metal, so that there is gap d between the film and the rod (Fig. 1).

The rod is illuminated by a plane electromagnetic wave incident normally on the metal film from above. In the absence of the rod, the electromagnetic field above the film surface ($x \geq 0$) is composed of the incident and reflected waves, so that the total electric field can be written as $\boldsymbol{E}_0(x) = \boldsymbol{E}_{0i}\left(e^{-ik\sqrt{\varepsilon_D}x} + re^{ik\sqrt{\varepsilon_D}x}\right)$, where $r = \left(\sqrt{\varepsilon_D} - \sqrt{\varepsilon_{Me}}\right) / \left(\sqrt{\varepsilon_D} + \sqrt{\varepsilon_{Me}}\right)$ is the Fresnel reflection coefficient of the film surface, ε_{Me} is the permittivity of the film material. Inside the metal film, the electric field is given by $\boldsymbol{E}_0(x) = t\boldsymbol{E}_{0i}e^{-ik\sqrt{\varepsilon_{Me}}x}$, where $t = 2\sqrt{\varepsilon_D} / \left(\sqrt{\varepsilon_D} + \sqrt{\varepsilon_{Me}}\right)$ is the Fresnel transmission coefficient of the dielectric-metal boundary (the factor $e^{-i\omega t}$ in the above expressions is implied, but not written explicitly). The nanoantenna modifies the distribution of the electromagnetic field due to its induced polarization. If it were not for the surface dressing effect, then within the electrostatic approximation valid for a rod of small radius, under the influence of the primary ($E_0(x)$) field, the rod would acquire a dipole moment (DM) given by $\boldsymbol{p}_0^{Cyl} = 2V_{Cyl}\varepsilon_0\varepsilon_D\left(\varepsilon_{Me} - \varepsilon_D\right)\boldsymbol{E}_0(x_0) / \left(\varepsilon_{Me} + \varepsilon_D\right)$, where $V_{Cyl} = \pi r_{Cyl}^2 l_{Cyl}$ is the volume of the rod. To explain the surface dressing effect [40] we represent the polarization charges separated in the rod as point charges (more precisely, in 2D geometry, these correspond to infinitely long and thin charged threads). Both of these charges are imaged in the metal film, and the image charges generate an inhomogeneous electric field (Fig. 1(b)) causing the nanoantenna to acquire both additional dipole and multipole moments of higher orders. The amount of the additional DM will be equal to $\boldsymbol{p}_1^{Cyl} = q_C\boldsymbol{p}_0^{Cyl}$, where $q_C = \left(\frac{r_{Cyl}(\varepsilon_{Me}-\varepsilon_D)}{2x_0(\varepsilon_{Me}+\varepsilon_D)}\right)^2$. With the dipole moment $\boldsymbol{p}_1^{Cyl}$, one can associate additional polarization charges in the rod, which will again be imaged in the film and induce a new additional contribution to the DM of the nanoantenna, and so on to infinity. By summing up the corresponding geometric progression, the resulting dipole moment of the rod is found to be

$$\boldsymbol{p}^{Cyl} = F_A^{Cyl}\boldsymbol{p}_0^{Cyl} \tag{3}$$

where $F_A^{Cyl} = \frac{1}{1-q_C}$ is the dipole moment amplification factor due the image charges in the film.

It should be noted that the accuracy of expression (3) will be lower for small gaps $d \ll r_{Cyl}$, since in this case the image multipoles of higher orders will affect the magnitude of the dipole moment of the rod, which we will, however, neglect for simplicity. Simplifying the problem further, we replace the rod with a 2D point dipole with dipole moment magnitude specified by expression (3). Then the amplitude of the SPP mode can be obtained simply by replacing p_0 with p^{Cyl} in expression (2). In particular, for the z-component of the SPP amplitude at the sur-

face of the film, we have

$$E_{0z}^{SPP} = -\gamma_{Vac}^2 \left| \frac{\varepsilon_{Me}^{3/2}\varepsilon_D^{3/2}}{\varepsilon_{Me}^2 + \varepsilon_D^2} \right| 2\pi r_{Cyl}^2 \frac{\varepsilon_{Me} - \varepsilon_D}{\varepsilon_{Me} + \varepsilon_D} \quad (4)$$
$$F_A^{Cyl}\, exp(-\gamma_{Vac} x_0) E_0(x_0)$$

The amplitude of component E_{0z}^{SPP} calculated as a function of the gap between the film and rod, of the nanoantenna radius, and of the wavelength is shown, correspondingly, in Figs. 3–5. The solid curves in these figures represent the analytical calculations in accordance with expression (4), and the numerical results are shown with the dots. We assume again $\varepsilon_D = 1$ for simplicity.

One can see from Fig. 3 that all analytical dependences $E_{0z}^{SPP}(d)$ show a sharp decrease in SPP amplitude at the beginning of the curves, while those calculated numerically for $\lambda = 550$ nm and $\lambda = 600$ nm first rise steeply (when the gap is below ~3 nm and ~ 1.5 nm, respectively, as illustrated by the insets in Fig. 3) and only then decrease. This difference is due to neglecting higher-order multipole moments in the analytical calculations. The effect of multipoles is, however, very "short-range" and plays a significant role only at the smallest gaps. For larger values of d, as can be seen from Fig. 3, the analytical and numerical results are in close agreement. We also note that for $\lambda = 650$ nm (curve 3) no disagreement between the analytical and numerical results is observed near $d = 0$, which can be explained as follows. The efficiency of excitation of higher-order local plasmon modes (quadrupole, octupole, etc.) in cylindrical nanoantennas usually decreases sharply with increasing the wavelength-to-radius ratio [46]. The effect of multipole moments is, therefore, evident only for the "short-wavelength" dependences 1 and 2 and not for the more "long-wavelength" dependence 3. A further sharp decrease in the SPP mode amplitude with increasing gap d for all three calculated dependences is explained by the rapidly weakening effect of the image charges on the

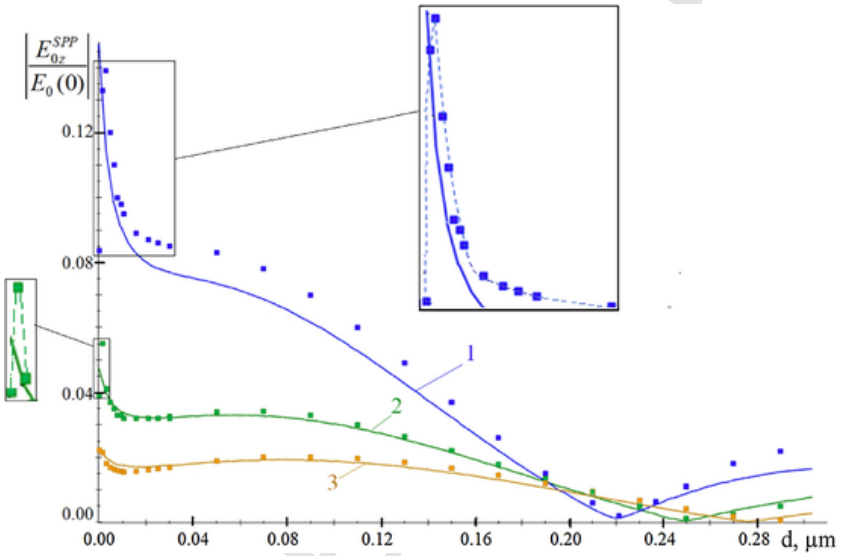

Fig. 3. Calculated dependences of the amplitude of the longitudinal component of the SPP electric field normalized to the amplitude of the primary wave at the film-vacuum interface $E_0(0)$ on the gap between the nanoantenna and the film. The analytical (solid curves) and numerical (dots) results are shown for $r_{Cyl} = 20$ nm, $\varepsilon_D = 1$, and $\lambda = 550$ nm (1), $\lambda = 600$ nm (2), $\lambda = 650$ nm (3). To emphasize the difference between analytical and numerical results near $d = 0$, the corresponding sections of dependences 1 and 2 are shown in the insets on an enlarged scale with the numerical results interpolated with dashed lines.

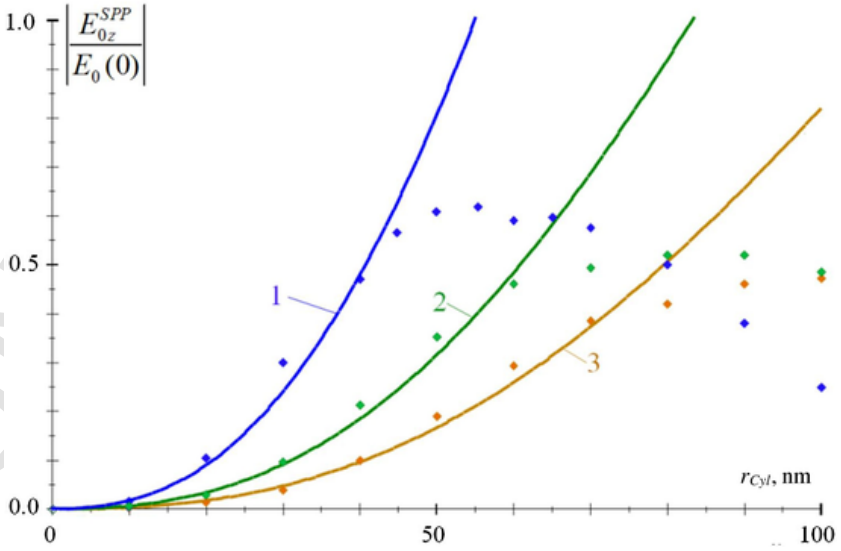

Fig. 4. The calculated dependences of the amplitude of the longitudinal component of the SPP electric field normalized to the amplitude of the primary wave at the film-vacuum interface $E_0(0)$ on the radius of the cylindrical nanoantenna. The solid curves represent analytically calculated results for $d = 10$ nm, and $\varepsilon_D = 1$, and $\lambda = 550$ nm (1), $\lambda = 600$ nm (2), $\lambda = 650$ nm (3). The corresponding numerical results are shown with dots.

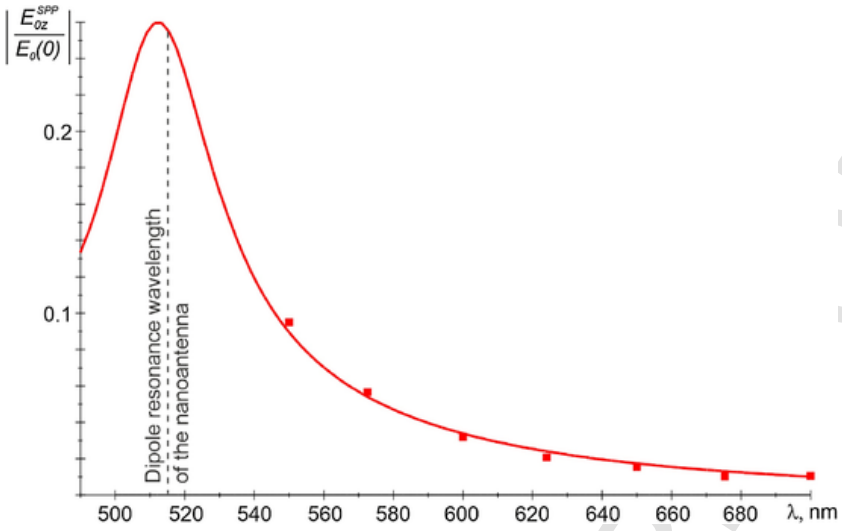

Fig. 5. The calculated dependences of the amplitude of the longitudinal component of the SPP electric field normalized to the amplitude of the primary wave at the film-vacuum interface $E_0(0)$ on the wavelength of the incident wave for d = 10 nm, ε_D = 1, and r_{Cyl} = 20 nm. The analytical and numerical results are shown with a solid curve and dots, respectively.

dipole moment of the nanoantenna, until the latter, upon reaching a certain threshold, is approximately equal to the dipole moment of an isolated thin rod in vacuum (in expression (3), the gain factor F_A^{Cyl} decreases rapidly with d and approaches unity at $d \sim 8$ nm (for $\lambda = 650$ nm), 10 nm (for $\lambda = 600$ nm) and 14 nm (for $\lambda = 650$ nm)). The decrease in the SPP amplitude then slows down significantly (curve 1 in Fig. 3) or can even change into a slight increase (curves 2, 3). Afterwards, the dependences acquire a damped quasiperiodic character. This behavior is explained by the fact that, on the one hand, the nanoantenna finds itself, with varying d, either in a maximum or minimum of the interference pattern produced by the incident and reflected waves (periodicity), and on the other hand, the effect of the nanoantenna on the electron plasma of the near-surface layer of the film decreases with increasing its height above the film according to the law $e^{-\gamma_{Vac} x_0}$ (damping).

The calculated dependences of the SPP amplitude on the radius of the nanoantenna are presented in Fig. 4 for a fixed gap d = 10 nm and three different excitation wavelengths. Such a value of the gap was chosen to avoid the effect of higher-order multipoles on the results of numerical calculations. It can be seen from the presented results that a quadratic growth of the SPP amplitude with r_{Cyl}, which follows from Eq. 4, agrees closely with the numerical calculations, so far as the radius of the rod is below ~ 45 nm at $\lambda = 550$ nm, ~ 55 nm at $\lambda = 600$ nm (2), and ~ 70 nm at $\lambda = 650$ nm. A significant discrepancy observed for larger radii is undoubtedly due to the limited applicability of the quasi-static approximation, which is guaranteed to be valid for $k\sqrt{\varepsilon_D} r_{Cyl} << 1$ and becomes increasingly inaccurate with the growth of this parameter [46].

The dependence of the SPP mode amplitude on the excitation wavelength (Fig. 5) was also calculated at $d = 10$ nm to minimize the effect of multipoles. As far as the numerical simulation is concerned, the lowest wavelength is chosen to be $\lambda = 550$ nm since at shorter wavelengths it is impossible to single out the surface plasmon wave against the background of the near and scattered field of the nanoantenna due to the huge propagation losses of SPP, which is what we do at longer wavelengths, as mentioned above. For analytical calculations, on the other hand, we took a smaller value of 490 nm so that the real part of gold permittivity is less than -1 in the entire calculation range. The latter is, in fact, the condition for the existence of the SPP mode at the gold – vacuum interface [44]. The upper limit of the calculation range was chosen so as to keep it in the visible part of the spectrum.

Another reason that we have chosen the lower boundary of the wavelength range for the analytical calculation some 60 nm to the left of that of the numerical simulation is to demonstrate a resonant peak in the analytic curve, which should be expected as a result of the dipole resonance of the nanoantenna. As seen from the figure, the peak is indeed observed near the wavelength of the dipole resonance of a thin gold rod in vacuum (marked with a dashed vertical line in Fig. 5). The slight spectral shift is most likely due to the effect of the substrate and has little to do with field delay phenomena, since the latter, as follows from the data presented in Fig. 4, are insignificant for a rod of such a small radius. It can also be seen from Fig. 5 that, within the spectral region where the numerical simulation was performed, there is good agreement between the numerical and analytical results, which confirms the validity of our analytical approach.

In conclusion, we have shown that the amplitude of SPP excited on a plane metal-dielectric interface by a nanoantenna can be analytically calculated using the method for calculation of guided-mode amplitudes in the presence of current sources widely used in the waveguide theory. The method gives good correspondence with the results of the full-wave numerical simulation as long as the nanoantenna can be described in the framework of the dipole approximation. For the visible range (500–650 nm), the developed method is applicable for the case of gold nanoantennas with the characteristic size up to 100 nm. It is worth mentioning that we considered two-dimensional geometry corresponding to the case of infinitely long nanoantennas (nanowires). Nevertheless, the proposed approach is also applicable to the 3D case, when the SPP is excited by a finite dipole particle, which will be the topic of our follow-up publication. We believe that the presented approach can be useful for modeling various phenomena associated with SPP excitation in plasmonics, micro- and nano-optics.

Declaration of Competing Interest

The authors declare that they have no known competing financial interests or personal relationships that could have appeared to influence the work reported in this paper.

Acknowledgement

This work was supported by the Russian Foundation for Basic Research under Grant 20-02-00556A.

References

[1] R. Wood, On a remarkable case of uneven distribution of light in a diffraction grating Spectrum, Proc. Phys. Soc. London 18 (1902) 269.

[2] U. Fano, The theory of anomalous diffraction gratings and of quasi-stationary waves on metallic surfaces (Sommerfeld's waves), J. Opt. Soc. Am. 31 (March 3) (1941) 213.
[3] R.H. Ritchie, Plasma losses by fast electrons in thin films, Phys. Rev. 106 (June 5) (1957) 874–881.
[4] J.A. Dionne, H.J. Lezec, H.A. Atwater, Highly confined photon transport in subwavelength metallic slot waveguides, Nano Lett. 6 (9) (2006) 1928–1932.
[5] V.J. Sorger, et al., Experimental demonstration of low-loss optical waveguiding at deep sub-wavelength scales, Nat. Commun. 2 (September 1) (2011) 331.
[6] S. Kawata, Y. Inouye, P. Verma, Plasmonics for near-field nano-imaging and superlensing, Nat. Photonics 3 (7) (2009) 388–394.
[7] R. Colombelli, et al., Far-infrared surface-plasmon quantum-cascade lasers at 21.5 μm and 24 μm wavelengths, Appl. Phys. Lett. 78 (18) (2001) 2620.
[8] Q. Hu, B.S. Williams, S. Kumar, H. Callebaut, S. Kohen, J.L. Reno, Resonant-phonon-assisted THz quantum-cascade lasers with metal–metal waveguides, Semicond. Sci. Technol. 20 (July 7) (2005) S228–S236.
[9] J.N. Anker, W.P. Hall, O. Lyandres, N.C. Shah, J. Zhao, R.P. Van Duyne, Biosensing with plasmonic nanosensors, Nat. Mater. 7 (June 6) (2008) 442–453.
[10] J. Homola, S.S. Yee, G. Gauglitz, Surface plasmon resonance sensors: review, Sensors Actuators B Chem. 54 (January 1–2) (1999) 3–15.
[11] K.M. Mayer, J.H. Hafner, Localized surface plasmon resonance sensors, Chem. Rev. 111 (6) (2011) 3828–3857.
[12] S. Kim, J. Jin, Y.-J. Kim, I.-Y. Park, Y. Kim, S.-W. Kim, High-harmonic generation by resonant plasmon field enhancement, Nature 453 (June 7196) (2008) 757–760.
[13] J. Lee, et al., Giant nonlinear response from plasmonic metasurfaces coupled to intersubband transitions, Nature 511 (July 7507) (2014) 65–69.
[14] G. Vampa, et al., Plasmon-enhanced high-harmonic generation from silicon, Nat. Phys. 13 (July 7) (2017) 659–662.
[15] C.E. Talley, et al., Surface-enhanced Raman scattering from individual Au nanoparticles and nanoparticle dimer substrates, Nano Lett. 5 (August 8) (2005) 1569–1574.
[16] D. McFarland, M.A. Young, J.A. Dieringer, R.P. Van Duyne, Wavelength-scanned surface-enhanced raman excitation spectroscopy, J. Phys. Chem. B 109 (June 22) (2005) 11279–11285.
[17] M.S. Tame, K.R. McEnery, Ş.K. Özdemir, J. Lee, S.A. Maier, M.S. Kim, Quantum plasmonics, Nat. Phys. 9 (June 6) (2013) 329–340.
[18] M.L. Andersen, S.ø. Stobbe, A.S. Sørensen, P. Lodahl, Strongly modified plasmon–matter interaction with mesoscopic quantum emitters, Nat. Phys. 7 (March 3) (2011) 215–218.
[19] Jiří Homola, Marek Piliarik, Surface plasmon resonance (SPR) sensors, Surface Plasmon Resonance Based Sensors, Springer, Berlin, Heidelberg, 2006, pp. 45–67.
[20] G. Brolo, Plasmonics for future biosensors, Nat. Photonics 6 (November 11) (2012) 709–713.
[21] K.F. MacDonald, Z.L. Sámson, M.I. Stockman, N.I. Zheludev, Ultrafast active plasmonics, Nat. Photonics 3 (January 1) (2009) 55–58.
[22] J.A. Schuller, E.S. Barnard, W. Cai, Y.C. Jun, J.S. White, M.L. Brongersma, Plasmonics for extreme light concentration and manipulation, Nat. Mater. 9 (March 3) (2010) 193–204.
[23] M. Kauranen, A.V. Zayats, Nonlinear plasmonics, Nat. Photonics 6 (November 11) (2012) 737–748.
[24] J.M. Pitarke, V.M. Silkin, E.V. Chulkov, P.M. Echenique, Theory of surface plasmons and surface-plasmon polaritons, Rep. Prog. Phys. 70 (1) (2007) 1–87.
[25] G. Lévêque, O.J.F. Martin, Optimization of finite diffraction gratings for the excitation of surface plasmons, J. Appl. Phys. 100 (December 12) (2006) p. 124301.
[26] Otto, Excitation of nonradiative surface plasma waves in silver by the method of frustrated total reflection, Zeitschrift fur Phys. 216 (1968) 398–410.
[27] E. Kretschmann, H. Raether, Notizen: radiative decay of non radiative surface plasmons excited by light, Zeitschrift f{ü}r Naturforsch. A 23 (12) (1968) 2135–2136.
[28] D.V. Permyakov, I.S. Mukhin, I.I. Shishkin, A.K. Samusev, P.A. Belov, Y.S. Kivshar, Mapping electromagnetic fields near a subwavelength hole, JETP Lett. 99 (August 11) (2014) 622–626.
[29] J. Renger, S. Grafström, L.M. Eng, Direct excitation of surface plasmon polaritons in nanopatterned metal surfaces and thin films, Phys. Rev. B - Condens. Matter Mater. Phys. 76 (4) (2007) 1–7.
[30] C. Zhao, J. Zhang, Y. Liu, Light manipulation with encoded plasmonic nanostructures, EPJ Appl. Metamaterials 1 (December) (2014) 6.
[31] D. O'Connor, P. Ginzburg, F.J. Rodriguez-Fortuno, Ga. Wurtz, a.V. Zayats, Spin-orbit coupling in surface plasmon scattering by nanostructures, Nat. Commun. 5 (2014) 5327.
[32] F.J. Rodriguez-Fortuno, et al., Near-field interference for the unidirectional excitation of electromagnetic guided modes, Science (80-.) 340 (April 6130) (2013) 328–330.
[33] A. Krasnok, S. Li, S. Lepeshov, R. Savelev, D.G. Baranov, A. Alú, All-Optical Switching and Unidirectional Plasmon Launching with Nonlinear Dielectric Nanoantennas, Phys. Rev. Appl. 9 (January 1) (2018) p. 014015.
[34] M.I. Petrov, S.V. Sukhov, A.A. Bogdanov, A.S. Shalin, A. Dogariu, Surface plasmon polariton assisted optical pulling force, Laser Photon. Rev. 10 (January 1) (2016) 116–122.
[35] F. Bigourdan, J.-P. Hugonin, F. Marquier, C. Sauvan, J.-J. Greffet, Nanoantenna for electrical generation of surface plasmon polaritons, Phys. Rev. Lett. 116 (March 10) (2016) p. 106803.
[36] L. Dvoretckaia, K. Ladutenko, A. Mozharov, G. Zograf, A. Bogdanov, I. Mukhin, Electrically driven metal and all-dielectric nanoantennas for plasmon polariton excitation, J. Quant. Spectrosc. Radiat. Transf. 244 (March) (2020) p. 106825.
[37] A. Andryieuski, et al., Direct characterization of plasmonic slot waveguides and nanocouplers, Nano Lett. 14.7 (2014) 3925–3929.
[38] Sinev, F. Komissarenko, I. Iorsh, D. Permyakov, A. Samusev, A. Bogdanov, Steering of guided light with dielectric nanoantennas, ACS Photonics (February) (2020) p. acsphotonics.9b01515.
[39] S. Sinev, et al., Chirality driven by magnetic dipole response for demultiplexing of surface waves, Laser Photon. Rev. 11 (September 5) (2017) p. 1700168.
[40] B. Evlyukhin, S.I. Bozhevolnyi, Point-dipole approximation for surface plasmon polariton scattering: implications and limitations, Phys. Rev. B 71 (April 13) (2005) p. 134304.
[41] T. Søndergaard, S.I. Bozhevolnyi, Surface plasmon polariton scattering by a small particle placed near a metal surface: an analytical study, Phys. Rev. B - Condens. Matter Mater. Phys. 69 (4) (2004) 1–10.
[42] Allan W. Snyder, John D. Love, Optical Waveguide Theory, Publisher: Chapman and Hall, 1983 734 p..
[43] S.A. Maier, Plasmonics: Fundamentals and Applications, Springer Science & Business Media, 2007.
[44] Lukas Novotny, Bert Hecht, Principles of Nano-Optics, Publisher: Cambridge University Press, 2006 537 p..
[45] W.M. Haynes, CRC Handbook of Chemistry and Physics, CRC press, 2014.
[46] Max Born, Emil Wolf, Principles of Optics, Publisher: Cambridge University Press, 1999 854 p..